11A.4 AN ANALYSIS OF DEEP CONVECTION INITIATION ENVIRONMENTS

Noah A. Lock* and Adam L. Houston

University of Nebraska-Lincoln, Lincoln, NE

1. INTRODUCTION

Fundamentally, deep convection initiation (DCI) requires that a volume of air be lifted to a level where it is able to realize considerable positive buoyancy over a significant depth. Positive area on a thermodynamic diagram for some lifted parcel is a necessary condition; however, the effects of dilution on the buoyancy that an actual updraft is able to realize cannot be neglected (Houston and Niyogi 2007; hereafter HN07). Also, the amount of lift that is needed depends on the amount of inhibition present below the level of free convection (LFC). These ideas are captured by the three "ingredients" of Johns and Doswell (1992) – instability, moisture, and lift. Consideration of the processes that govern convection suggests a slight modification to that approach in which DCI is examined in the context of two pairs of factors – buoyancy and dilution, and lift and inhibition. The "moist layer of sufficient depth" (Johns and Doswell 1992) has two roles. The first is to produce a parcel with sufficient θ_e to achieve positive buoyancy given the temperature profile and the assumptions of parcel theory. The second role (and primary reason the depth of the moisture is important) is to limit the dilution of the parcel as it ascends. Therefore, we contend that it is better to consider buoyancy and dilution as the governing factors. Furthermore, HN07 showed that a positive feedback exists between dilution and buoyancy. Lift and inhibition are paired since the amount of inhibition is what determines if a given amount of lift is sufficient to initiate a thunderstorm.

Buoyancy and inhibition are frequently assessed using parameters based on parcel theory, in particular convective available potential energy (CAPE; Moncrieff and Miller 1976) and convective inhibition (CIN). However, the collocation of significant CAPE and minimal CIN does not guarantee that deep convection will develop, even when a lifting mechanism is present (Ziegler and Rasmussen 1998; hereafter ZR98).

Lift of sufficient strength and depth to get the parcel to its LFC is assumed in the calculation of parameters based on parcel theory, including CAPE and CIN. Vertical motion is a quantity that is difficult to accurately diagnose in the atmosphere, due largely to sparse and flawed observational data. It has been known for quite some time that convergence lines are favored locations for convective initiation (Purdom 1982; Wilson and Schreiber 1986). Horizontal mass convergence at low levels creates pressure excesses near the ground and an associated upward pressure gradient force. This pressure gradient force will result in upward acceleration of air parcels that could be sufficient to get them to their LFC. Accordingly, low-level convergence is often used as a measure of lift in forecasting DCI, and airmass boundaries are favored locations for this to occur.

The explicit exclusion of parcel dilution is one of the major limitations of traditional parcel theory. Dilution occurs when a rising parcel entrains environmental air with lower θ_e, which acts to reduce the amount of buoyancy the parcel can realize. Entrainment of environmental air can affect the parcel in two ways. One is the reduction of parcel θ_e by mixing it with environmental air with lower θ_e. This process is relevant to both saturated and unsaturated parcels. Another process that affects saturated parcels is evaporation brought about by mixing with dry environmental air, which acts to cool the parcel. The theory of criticality proposed by HN07 is an effort to include the feedback between buoyancy and parcel dilution in the process of convection initiation. In their numerical experiments, deep convection only occurred if the rate at which parcels could gain buoyancy through ascent exceeded the rate at which buoyancy was lost through dilution. The presence or absence of deep convection was found to be related to the lapse rate of the active cloud-bearing layer (ACBL), which is the layer above the LFC where "active" convection is occurring (Stull 1985).

* *Corresponding author address:* Noah A. Lock, Univ. of Nebraska – Lincoln, Dept. of Earth and Atmospheric Sciences, Lincoln, NE 68588; e-mail: nlock@huskers.unl.edu

Though dilution is a cumulus-scale process that cannot be directly measured or computed from the data available, environmental parameters relevant to dilution (humidity, ACBL lapse rate and wind shear) can be measured, and that is the intent here.

The purpose of this work is to determine how often each of the basic factors (buoyancy, dilution, lift, and inhibition) is the difference between thunderstorms initiating and thunderstorms not initiating. Even though the reasoning outlined above applies to deep convection in general, the data in this study are generated from a subset of deep convection that produced cloud-to-ground lightning. The most accurate description of this dataset is thunderstorms that produce cloud-to-ground lightning; however, in the interest of brevity, these will be described as "thunderstorms". This determination requires quantifying the factors at locations where initiation occurred as well as other locations where initiation did not occur as a point of comparison. These locations need to be related enough to make meaningful pairwise comparisons. To quantify the factors, a number of parameters will be computed from RUC-II model analysis data (Benjamin et al. 2004; NCDC 2011a), with the intent that they be independent of geography and/or season as much as possible. To be clear, the use of parameters is not intended as a search for an as-yet-undiscovered "magic bullet" to forecast thunderstorm initiation. Rather, the relative importance of a parameter is used to indicate the importance of the factor it is measuring. Since multiple parameters may be used to measure the same basic factor, some insight can be gained on the most effective ways of quantifying each factor.

2. DESCRIPTION OF PARAMETERS

Though an essentially infinite range of parameters could be computed from RUC-II data, the parameters chosen for this study are intended to represent physical processes occurring in the environment that would affect the development of convection. The parameters to be computed from the RUC-II analysis data are shown in Table 1. The descriptions and justifications for the parameters used in this work follow.

Table 1: Parameters to be computed from RUC-II analysis data, listed by basic factors the parameters are designed to quantify.

Lift and Inhibition	**Buoyancy and Dilution**
CIN	CAPE
Maximum omega	ACBL lapse rate
Ht of maximum omega	LCL-LCL+2km CAPE
H_{LFC}	0 to top of ACBL mixing ratio difference
Convergence	ACBL wind shear
Subcloud wind shear	
Δz^*	

CIN. One of the most commonly used metrics to forecast initiation is CIN, as it quantifies how much lift must be provided for a parcel to reach its LFC. There are three main "parcels" that are commonly used to compute CIN (and CAPE) – the surface parcel, the mixed-layer parcel, and the most unstable parcel. Here all three will be used with the purpose of comparing the outputs to evaluate the assumptions made about the properties of the parcels responsible for initiating thunderstorms. The surface-based method assumes the parcels that initiate convection mainly originate near the surface. This assumption is clearly inadequate for cases of elevated convection, where convection occurs above a low-level inversion. The most-unstable parcel method assumes that the parcels with the highest θ_e are most relevant. In many cases, the surface-based and most-unstable methods are equivalent since the surface parcel is the one with the highest θ_e. The mixed-layer method uses a "parcel" with the mean mixing ratio and potential temperature of the lowest 100 mb or lowest 1 km of the atmosphere (here the lowest 100 mb layer is used). This method is an attempt to account for mixing within the boundary layer, and it generally yields more conservative values of CAPE and CIN than the other methods. The virtual temperature correction (Doswell and Rasmussen 1994) is used in all parcel-based calculations. It is hypothesized in this work that there will be significantly less CIN in cases with storms, though there will also be null cases with minimal CIN, and that a combination of CIN with information about the lift present will be more useful.

Maximum omega and height of maximum omega. Lift is one of the important factors for the formation of thunderstorms. In the past, estimates of vertical motion were not available at the spatial and temporal resolution needed for forecasting thunderstorm

initiation, so vertical motion was assumed or inferred from other fields. With the advent of the RUC and other similar models, estimates of vertical motion are available at 20-km grid spacing and hourly resolution. While this grid spacing is unable to resolve meso-γ scale updrafts that directly initiate thunderstorms, it is worth testing the ability of this parameter to discriminate environments that do or do not initiate thunderstorms. Specifically, both the magnitude of maximum upward motion no higher than 100 mb above the LFC and the height of that maximum value will be obtained from the RUC-II data, as both the strength and depth of lift may be relevant to initiation. It is hypothesized that both will be higher where initiation occurred. Additionally, the height of maximum upward motion is needed to compute H_{LFC}, which is described next.

H_{LFC}. As described by ZR98, H_{LFC} is the ratio of the height of maximum upward motion (assumed to represent the top of the mesoscale updraft) and the height of the LFC. Values significantly greater than 1 suggest that initiation will occur since parcels are being lifted above their LFC. This ratio combines information about the depth of lift present and information about the depth of lift needed, so it is hypothesized that it will be quite effective in assessing the potential for thunderstorm initiation. However, the effectiveness of the metric is dependent on the quality of the vertical motion information available from the RUC.

Convergence. Many studies (e.g. Wilson et al. 1992; Xue and Martin 2006) have related DCI to areas of enhanced convergence. The depth of convergence has also been shown to be important (Wilson et al. 1992; ZR98), thus, the convergence over a deeper layer (such as parcel level to LFC) may be more useful than surface convergence alone. The computation of both surface and 0-LFC mean convergence will allow this hypothesis to be tested. The 0-LFC mean convergence is the integral of convergence from the parcel level to the LFC for the most unstable parcel, divided by the distance between the two levels. The continuity equation relates vertical motion to the divergence, and vertical motion at a given level is the integral of the divergence in the level below it. Though moisture flux convergence is frequently used in the forecasting of severe storms, Banacos and Schultz (2005) suggest that simple mass convergence provides essentially the same information and is more physically sound. However, as noted by Doswell and Schultz (2006), divergence can be a rather noisy and volatile field due to sparse and potentially erroneous observations.

Subcloud wind shear. RKW theory (Rotunno et al. 1988) states that when the horizontal vorticity associated with the cold pool is equal and opposite the environmental vorticity strong vertical updrafts are created along the gust front. Though originally conceived to explain squall line maintenance, the basic physical principles can still be applied for thunderstorm initiation (Lee et al. 1991). Since we are interested in "first initiation", there should be no "cold pools", though there could be airmass boundaries, which have horizontal vorticity associated with them. Accordingly, the idea of environmental vorticity due to vertical wind shear balancing the vorticity associated with the airmass boundary to create enhanced updrafts along the boundary seems plausible. This idea was lent some credence by Lee et al. (1991), who evaluated a case of thunderstorm initiation along colliding boundaries and found that the removal of low-level shear in a model simulation diminished the convection. Here low-level shear is defined as shear between the parcel level and the LCL in order to represent subcloud shear and to be able to account for elevated parcels. It is hypothesized that increased subcloud shear is favorable for initiation.

Δz^*. First introduced by HN07, this measures how large a vertical displacement is needed for a parcel to reach its LFC. This is useful since it is related to the depth of lift needed to initiate a thunderstorm instead of just the strength of the lift. It is hypothesized that smaller values of Δz^* will be found in cases with storms.

CAPE. The existence of positive CAPE is a necessary, but not sufficient, condition for thunderstorms to occur. In theory, more CAPE would produce a stronger updraft given that the parcel is able to reach the LFC. Similar reasoning as for CIN applies to the use of surface-based, mixed-layer, and most-unstable parcels to compute CAPE. It is hypothesized that there will be a significant overlap in the distributions of CAPE in the storm and no storm categories, making CAPE of little use in discriminating initiation and non-initiation environments.

ACBL lapse rate. This parameter was shown to be important in the success or failure of DCI by HN07 (here the ACBL is defined as a 1.5 km deep layer starting at the LFC). As concluded by HN07, larger lapse rates increase the vertical displacement of parcels caused by an airmass boundary due to reduced static stability. Also, steeper lapse rates above the LFC allow parcels ascending through the layer to gain buoyancy more rapidly. Parcels for which the gain of buoyancy through ascent exceeds the loss of buoyancy through

entrainment are termed “supercritical” by HN07. The hypothesis of this work is that lapse rates will be larger in environments that initiate thunderstorms.

LCL-LCL+2km CAPE. This has been developed specifically for this work and is defined analogously to CAPE and CIN in height coordinates, except the limits of integration are the LCL and 2 km above the LCL. The depth of the layer was chosen to represent the region immediately above the cloud base where the feedback between buoyancy and dilution is most important. Since the sign of the virtual temperature difference may be either positive or negative in this layer, both positive and negative values are meaningful. Positive values indicate there is more CAPE than CIN in the layer, while negative values indicate the opposite. The purpose of this metric is to quantify how quickly a parcel can gain buoyancy. It is hypothesized that the distribution of CAPE within the sounding is important, with more CAPE in the low levels of the sounding being more supportive of initiation since parcels are more able to overcome the negative effects of dilution. Though this effect is also measured by the ACBL lapse rate, a CAPE framework takes parcel moisture into account.

0 to top of ACBL mixing ratio difference. This is another parameter developed specifically for this work. It is designed to represent the cumulative potential entrainment a rising parcel might experience as it ascends to a level where it is significantly buoyant. The relevant quantity to measure the dryness of the environment relative to the parcel is the difference between parcel mixing ratio and environmental mixing ratio. By integrating this quantity from the parcel level to the top of the ACBL, the overall dryness of the environment during the critical early stages of convective development can be characterized. Though entrainment is known to be an important process in the evolution of convection, it is neglected by parcel theory and not very well understood. Ziegler et al. (1997) showed that in mesoscale updrafts along a dryline where thunderstorms develop the change in mixing ratio from the surface to the LFC is minimal, in contrast to nearby areas where they do not develop. This deepening of the moist layer is a result of persistent convergence and upward motion. It is hypothesized that if rising parcels must pass through deep dry layers before significant buoyancy is achieved then the likelihood of thunderstorm initiation will be reduced.

ACBL wind shear. While vertical wind shear is known to help in storm organization and severity, a number of studies have suggested that vertical shear above the boundary layer has a negative effect on storm initiation. Weisman and Klemp (1982) and Lee et al. (1991) showed that increased vertical shear tended to decrease the maximum updraft speed of the convection and delay its onset. Possible mechanisms by which increased shear above the LFC can inhibit convection are increased entrainment and the advection of developing clouds away from the boundary layer updraft. Entrainment is a turbulent mixing process, and greater wind shear leads to greater turbulence, so greater wind shear may lead to increased entrainment. Wind shear also tilts the updraft, increasing the surface area subject to entrainment. For a mesoscale updraft to initiate a thunderstorm, rising parcels need to reach their LFC before being advected out of the updraft region (ZR98). Peckham and Wicker (2000) showed that stronger cross-dryline flow in the 0-5 km layer inhibited the growth of deep convection along the dryline since clouds were more rapidly advected away from the surface-based convergence band associated with the dryline. If sufficient dynamic perturbation pressure gradients were not yet established, then the incipient storms fell apart. It is hypothesized that there will be less wind shear in the ACBL in the cases of deep convection. The notion of wind shear having opposite effects depending on the layer of the shear is consistent with the results of Lee et al. (1991). For both this parameter and the subcloud wind shear parameter, the orientation of the shear with respect to a possible mesoscale boundary is relevant in addition to the magnitude of the shear. A limitation of the present analysis is that it is unable to consider the orientation of boundaries and only considers the magnitude of the shear.

3. METHODOLOGY

3.1. Radar-based Thunderstorm Identification

Accurately identifying locations where thunderstorms initiated and where they did not requires first identifying and tracking individual thunderstorms. For a large spatial domain covered by multiple radars, this is best done by combining the radar data into a common grid and identifying and tracking thunderstorms within that grid. Level-II radar data were downloaded from the NCDC archive (NCDC 2011b) for 2005-2007 for 44 radars covering the Great Plains (Fig. 1). The Thunderstorm Observation by Radar (ThOR; Lahowetz et al. 2010) algorithm was used to identify thunderstorm

tracks from these data. ThOR consists of the following key steps: 1) remove non-meteorological echoes using a neural network quality control algorithm (the w2qcnn algorithm of Lakshmanan et al. 2007a); 2) merge the data from individual radars into a common three-dimensional grid (the w2merger algorithm of Lakshmanan et al. 2006); 3) attenuate stratiform precipitation using fuzzy logic; 4) identify candidate thunderstorms through image segmentation of radar reflectivity to form reflectivity clusters (the w2segmotionll algorithm described by Lakshmanan et al. 2009); 5) track these clusters over time; 6) associate lightning to clusters along the tracks to classify tracks as thunderstorms. The w2qcnn, w2merger, and w2segmotionll algorithms are included in the Warning Decision Support Services – Integrated Information (WDSS-II; Lakshamanan et al. 2007b) package.

The horizontal extent of the grid used by w2merger is shown by the black box in Fig. 1. The grid spacing was 0.014° latitude x 0.011° longitude, approximately 1 km x 1 km.

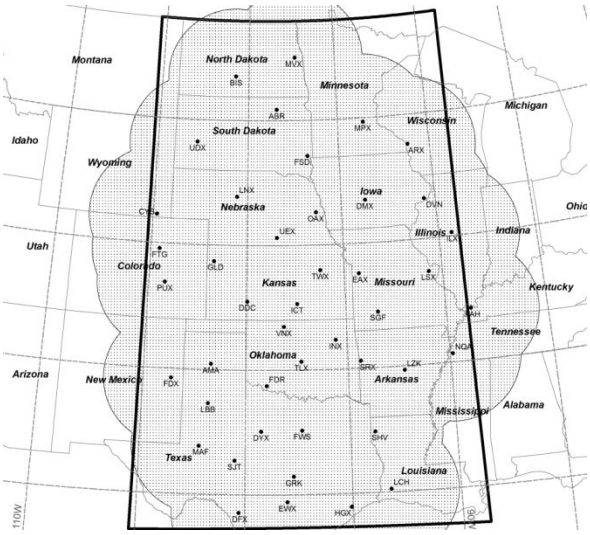

Figure 1: Map showing radars used in the study (labeled black dots), the area within 300 km of those radars (stippled), and the analysis domain (black box).

The w2segmotionll algorithm operated on the composite reflectivity fields (the maximum reflectivity within each vertical column) that were generated by w2merger at 5-minute granularity and subsequently modified by by the fuzzy logic algorithm. The reflectivity clusters identified by the w2segmotionll algorithm are constrained to have a composite reflectivity value between 30 and 70 dBZ and a minimum area of 50 km^2.

The algorithm to create tracks from the reflectivity clusters starts by identifying a cluster centroid that has not been placed on a track. The 0-6 km mean wind from the North American Regional Reanalysis (NARR; Mesinger et al. 2006; NCDC 2010) is used as the initial motion estimate for the first 10 minutes of each candidate track. After 30 minutes, the motion estimate is derived from the position history of the track; between 10 and 30 minutes the motion estimate is the weighted average of the NARR and position history estimates. Examining the observed clusters at subsequent times, the tracking algorithm creates all unique candidate tracks that begin at the given cluster. The candidate track with the lowest mean error (difference between actual position and projected position) over the duration of that candidate track is chosen as the correct track, provided that the candidate track contains at least two clusters.

The parameters that govern the behavior of the tracking algorithm, such as search radius, were determined by manually tracking thunderstorms from a variety of events and recording the search radius needed to follow the human tracks without allowing tracks to jump to another cluster when the correct track ended. Though there are inherent ambiguities in tracking thunderstorms (such as merging and splitting), the human tracks are intended to represent “best practices” in tracking. ThOR tracks were verified against both human tracks (different events than used for the training) and tracks produced by a benchmark tracking algorithm. The results indicated that ThOR matched the human tracks reasonably well, and outperformed the benchmark algorithm.

Cloud-to-ground lightning data are used to classify tracks as thunderstorms. Only those tracks that have at least one cluster at the same time and location as a strike are counted as thunderstorms (cluster positions and shapes are interpolated to account for the lightning data being at one-minute granularity and the clusters being at five-minute granularity). As mentioned above, the use of only cloud-to-ground lightning data will omit some legitimate thunderstorms from the dataset.

3.2. Identification of Initiation Points

From the final thunderstorm tracks output by ThOR, the times and locations of thunderstorm initiation can be determined. Since the first cluster on a track

represents the time at which sufficient radar reflectivity became present aloft, it is not exactly the time and location at which the updraft began. The initiation point to be used is found by extrapolating the storm's track backward 15 minutes from the appearance of the first cluster (Fig. 2a). These candidate initiation points are then checked to see if they are within a threshold distance, Δit, of "established" storms at the time of initiation (see Table 2 for the distance thresholds used for this work and Fig. 2b for a schematic of this procedure). "Established" storms are defined as thunderstorms that are at least 15 minutes old (30 minutes old when considering the backward extrapolation described above). Candidate initiation points beyond the threshold distance from established storms are retained. If a candidate initiation point is within the threshold distance, it is considered connected to the ongoing convection. As a result, the entire track is considered "established", and the initiation point is no longer considered. The primary interest of this study is the "first initiation" within an area, rather than initiation of new convective cells within an area where convection was already present, such as a pre-existing multicell system. The main reason for excluding initiations near existing storms is that established storms modify the environment at temporal and spatial scales that are not well-resolved by the available data (20-km RUC-II).

Table 2: Description of the distance thresholds and the values used in this study.

Threshold	Description	Value (km)
Δit	Threshold distance between candidate initiation point and "established" storm	100
Δii	Distance used to determine clustering of candidate initiation points	50
Δnt	Threshold distance between candidate null point and any thunderstorm location	40
Δni	Distance between initiation point and candidate null point	60, 120, 180

3.3. Selection of Points for Parameter Collection

3.3.1. Initiation Points

The initiation points remaining after the steps described in section 3.2 are grouped into hourly bins centered at the nominal RUC-II analysis times. The center of the bin is defined as t_0. Initiation points within Δii (Table 2) of each other are clustered into a single representative point. The method for determining which points should be grouped together is an adaptation of connected component analysis from graph theory (two points are considered "adjacent" if they are within Δii of each other). Within each group, the mean center of the group is defined as the mean latitude and mean longitude of all candidate initiation points in the group. The candidate initiation point nearest to this mean center is cataloged as the representative for this group (Fig. 2c). Candidate initiation points beyond Δii from all other initiation points ("isolated" initiations) are cataloged.

The motivation for this spatial grouping is to avoid biasing the final results by having many samples from the same location and time. This study is interested in whether a given environment produces deep convection, so whether one storm or five occur in that environment should not matter, and the sampling approach should reflect that. Similar reasoning was used by Thompson et al. (2003), who used time and space separation thresholds for their supercell climatology to avoid biasing their results to single events with a large number of supercells.

3.3.2. Null Points

In order to be most useful, the null cases chosen in this study need to represent an environment which is close to initiating convection, and maybe is missing just one ingredient. The strategy adopted in this study for selecting points to represent the null case environments takes points that are a distance Δni from the cataloged initiation points (Fig 2d). Only the candidate null points beyond a threshold distance Δnt from all thunderstorm locations within the hourly bin and Δni from all candidate initiation points within a 3-hour bin centered at t_0 are cataloged (Fig. 2d). This is to ensure that the selected null point is actually away from areas of convection. The reason a 3-hour buffer is used for initiation points is to avoid a situation where a sounding could be used to represent a "null point" in one bin and then be used as a t_{-1} initiation sounding for an initiation in the next hourly bin.

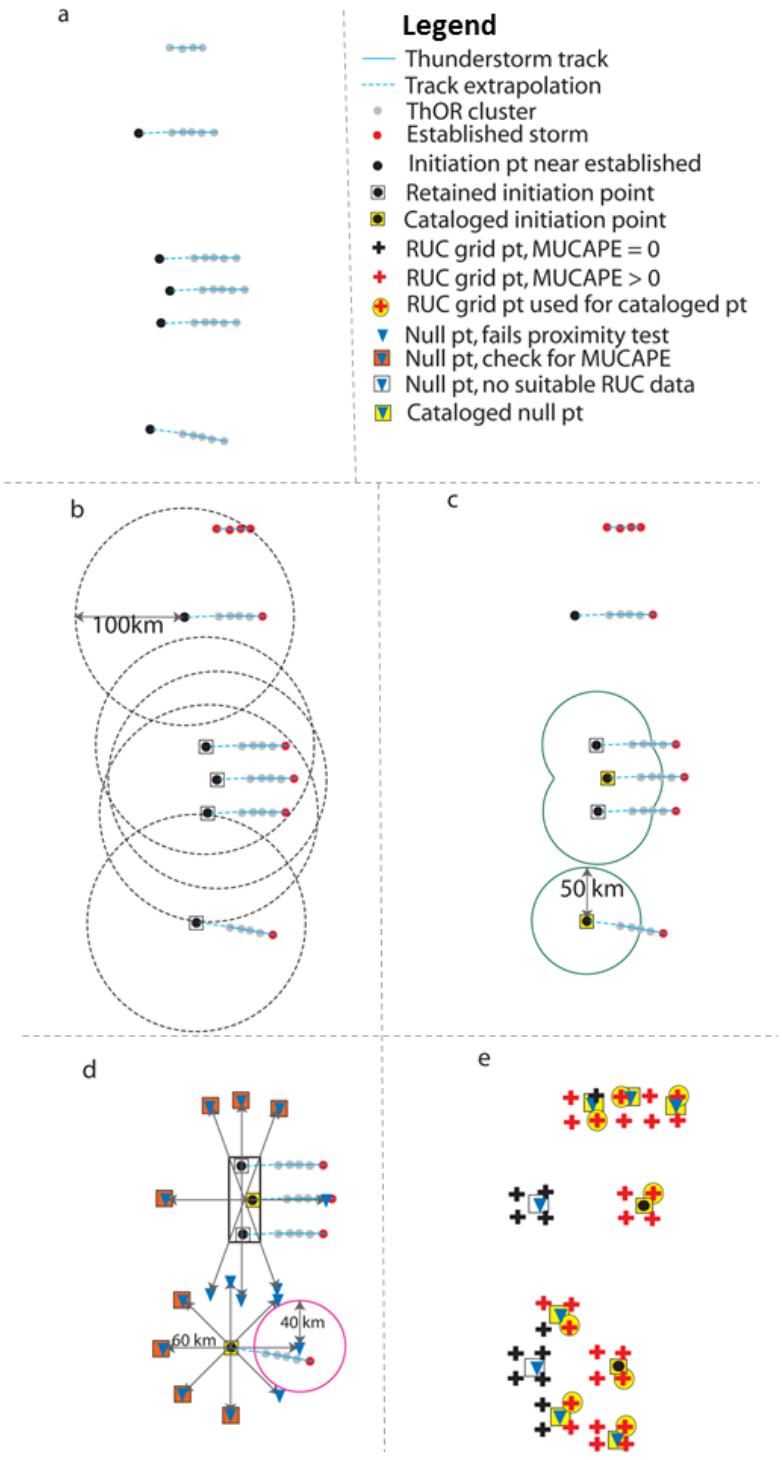

Figure 2: (a) Identification of initiation points by backward extrapolation of tracks. (b) Removal of initiation points within 100 km of established storms. (c) Spatial clustering of nearby initiation points. (d) Selection of locations to be used for null points. (e) Removal of points with no adjacent RUC grid points with positive MUCAPE.

There is some uncertainty concerning an appropriate value for Δni, as the most informative null points are those that are "close" to initiating convection and do not. As a result of the 20-km grid spacing and the method of selecting the model gridpoint used to compute the parameters, the minimum Δni to assure that under no circumstance could the initiation point and the null point use the same grid point is 60 km, so this was chosen as the minimum value of Δni (and the value that is used in Fig. 2). The other values of Δni are simply twice and triple this value.

For "isolated" initiation points, candidate null points are identified at a distance Δni from the initiation point in the 8 cardinal directions (Fig. 2d). For "grouped" initiation points, the shape of the group is approximated by a rectangle. The length of the rectangle is equal to the maximum distance between candidate initiation points in the group. The width of the rectangle is specified as twice the maximum distance from a candidate initiation point to the line connecting the maximally separated points. The actual latitude and longitude differences between those maximally separated points define the "rotation" of the rectangle. Candidate null points are then identified Δni from the corners of the rectangle and Δni from the midpoints of its sides (Fig. 2d). As the aspect ratio (length/width) of the rectangle becomes larger, the diagonal search directions compress toward the long axis of the rectangle. This is beneficial since a linear pattern of initiation points is likely along an atmospheric boundary of some kind, so the most useful null points will be those along the boundary that initiated the convection. Having more candidate null points near the boundary makes it more likely that the null points sampled will have environments near the initiation/non-initiation threshold, as these null points will be the most informative.

This approach assumes that the locations selected as null points have environments with many characteristics that support thunderstorm development; however, something is missing since thunderstorms did not develop there. Though this approach will likely reduce separation in distributions of parameter values between the two categories as the null environments are similar to the initiation environments, it should allow for the isolation of the "missing ingredients" in each case. This approach also allows pairwise differences to be used to compare storm and no storm cases, which is a way to eliminate event-to-event variability in the convective environments. This approach will be discussed further in Section 4.2.

3.4. Attribution of Parameter Values to Cataloged Points

The atmospheric parameters described in section 2 will be calculated from hourly RUC-II analysis using an NCAR Command Language (NCL) script. The RUC-II has a grid spacing of 20 km, and produces new analyses and forecasts every hour. As described by Benjamin et al. 2004, analysis fields are developed using the 1-hr forecast from the previous run as the "first guess". This first guess is then adjusted based on observations ingested from a variety of sources (for more details on the RUC-II data assimilation methods, see Benjamin et al. 2004). This "hot start" approach to developing analysis fields means that vertical motion has been "spun-up" at the analysis time.

The RUC grid point nearest the cataloged initiation or null point with positive most unstable CAPE (MUCAPE) will be used as the data source for that initiation or null point (Fig. 2e). The reason for this criterion is that positive MUCAPE is a necessary condition for deep convection to occur, and if the RUC grid point does not satisfy this condition then it is not a representative profile for an initiation point. This criterion is used for null points since the values of the other parameters are trivial if the necessary condition is not met. If the nearest grid point for a cataloged initiation or null point does not possess positive MUCAPE, the NCL script then checks the next nearest grid point for positive MUCAPE. The process continues until it finds a grid point with positive MUCAPE or it has searched the four nearest grid points, whichever is first. If none of the four nearest grid points meet the criterion, then that initiation or null point will not be used further. If a grid point has positive MUCAPE, then the script will compute the remaining parameters. The virtual temperature correction is used in all parcel-based computations. The parcel ascent is treated as a pseudoadiabatic process.

For the initiation and null points within each hourly bin, two data sets will be collected. The first will be from the analysis valid at the central time of the bin (t_0). These data are intended to represent the environment within 30 minutes either side of the observed initiation. The second data set will be from the previous hour's analysis (t_{-1}) and it is intended to represent the pre-initiation environment, since t_{-1} is at least 30 minutes before the observed initiation time.

4. RESULTS

4.1 Raw Values

The chosen method for analyzing the raw parameter values for initiation and null points is the box-and-whisker plot. For all box-and-whisker plots shown hereafter, the box represents the middle 50% of the data, the black line is the median, and the whiskers extend to the maximum data value within 1.5 times the interquartile range. Outliers beyond this range are not plotted. Null points at each range (60, 120, and 180 km) are shown along with the initiation points. The dataset contains 55,103 initiation points that are retained after the procedures described in section 3.2, and 324,000-352,000 null points (depending on range). This translates to an average of 6-7 null points at each range that can be paired with each initiation point, out of the 8 that were originally considered.

The plots of raw parameter values are shown in Fig. 3-4. One of the first things to notice is that all parameters show significant overlap between initiation and null distributions at all 3 ranges. This indicates that the spread in background environments overwhelms the differences between initiation and null points, and that thresholds that distinguish initiation from non-initiation for all cases do not exist. This is not surprising as the dataset includes both surface-based and elevated convection as well as a wide range of climate zones. This variation in environments should be most relevant to the thermodynamic variables, such as CAPE and Δz^*. It is somewhat surprising that a dimensionless variable such as H_{LFC}, which is designed to account for variation in environments, would not perform better at this stage. This means that more sophisticated pairwise analysis is required to extract useful information from this data (section 4.2).

Another characteristic of most variables is that the separation in medians increases as range increases, suggesting that the favorable convection initiation environment can be more skillfully identified at a precision of 180 or 120 km than 60 km. This is expected, as the scale of features resolvable by a model with 20-km grid spacing is ~80 km.

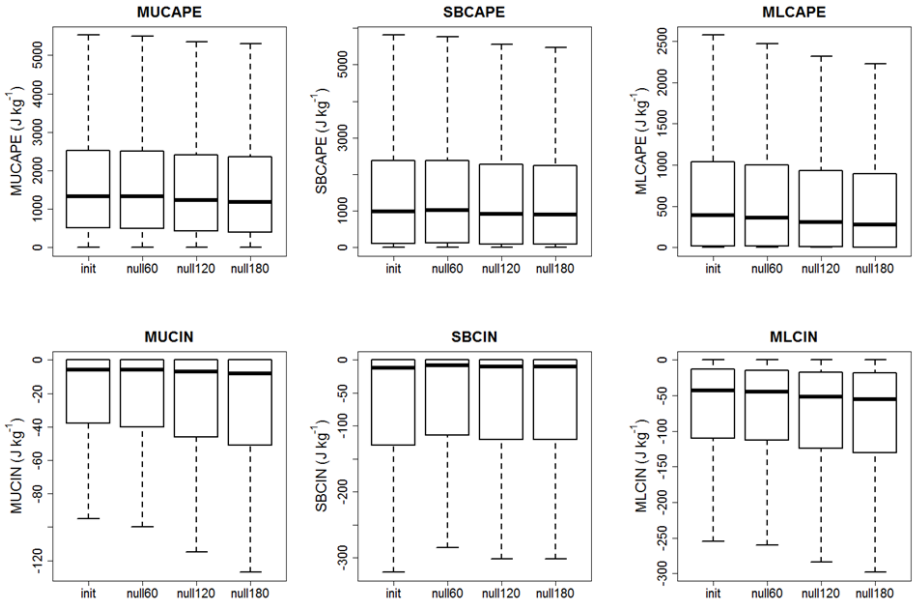

Figure 3: Box-and-whisker plots of raw CAPE and CIN values.

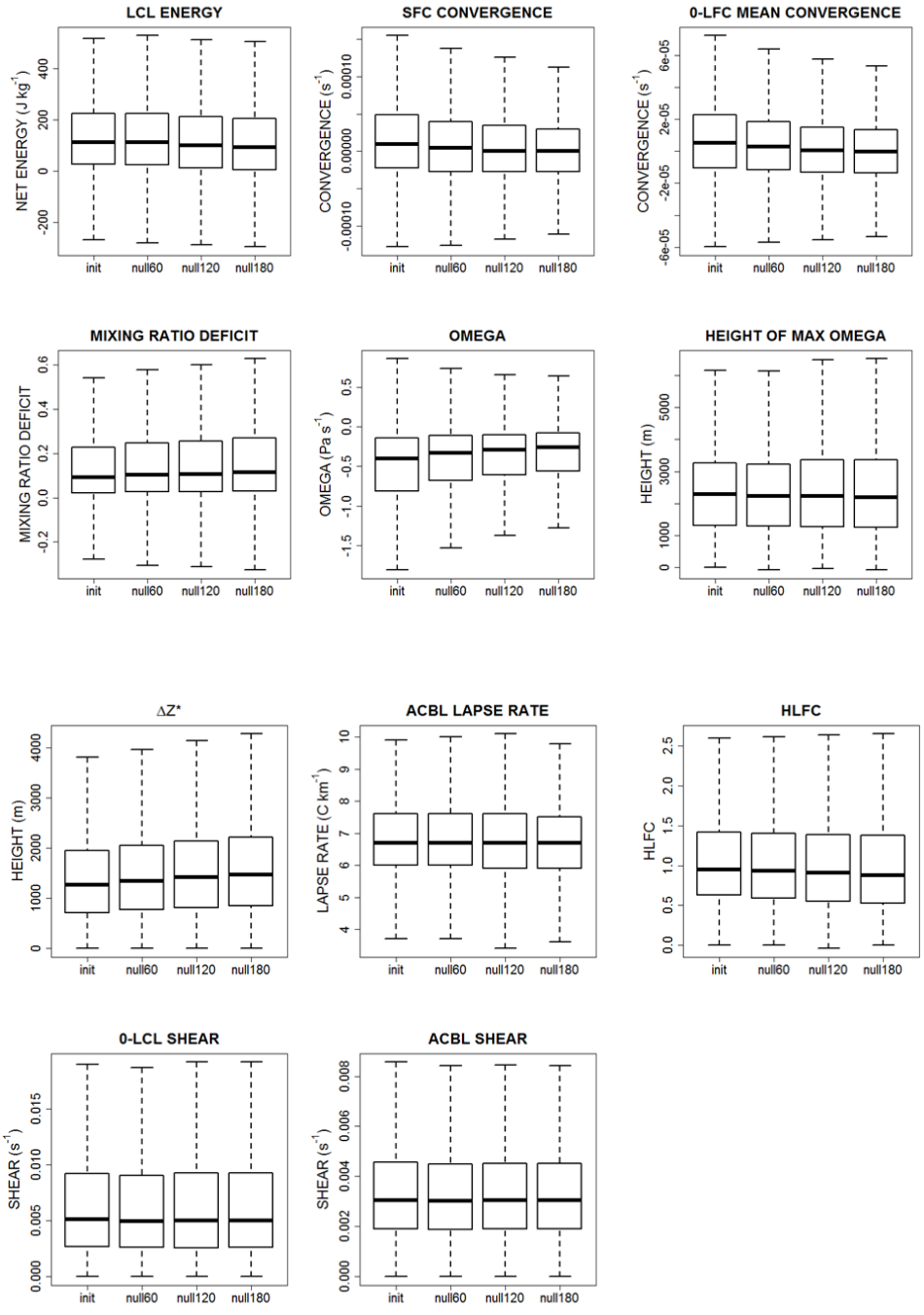

Figure 4: Box-and-whisker plots of raw values for remaining variables.

The approach used in this work to assess discriminatory ability from box-and-whisker plots is to evaluate the absolute value of the difference in medians divided by the interquartile range of the initiation point values. This quantity will hereafter be referred to as the

"separation". Applying this technique to the raw data shows that the parameters with the most discriminatory ability are maximum omega, convergence (both surface and 0-LFC), Δz*, and mixed-layer CAPE and CIN. The separation values for these parameters are shown in Table 3. Though the order of parameters is similar at each range, the values increase as the range increases. Shear values seem to make very little difference, as all four boxes are essentially identical for both 0-LCL and ACBL shear.

Table 3: Separation values for raw data at each range.

Range	Max omega	0-LFC conv	Sfc conv	Δz*	MLCIN	MLCAPE
60 km	0.10	0.08	0.07	0.06	0.02	0.03
120 km	0.16	0.14	0.14	0.12	0.09	0.08
180 km	0.21	0.18	0.17	0.17	0.12	0.11

4.2. Pairwise Differences

The goal of this work is to find the factor that is different between initiation and null points, so it is natural to consider the pairwise difference between an initiation point and the null points associated with it. All initiation and null points that do not have a "mate" with valid data are discarded at this stage. The same initiation point could be paired with as many as eight null points and differences were computed for each resulting pair. Absolute differences are transformed to a common scale to facilitate comparison of the discriminatory ability of each parameter. This transformation accounts for the relative magnitude of values being compared (a difference in CIN of 10 J kg^{-1} is much more significant when the raw values are -5 and -15 than when they are -90 and -100) and accounts for the possibility of one or both parameters being zero or negative. For this transformation the difference for initiation points is defined as

$$I = \frac{init - null}{\max(abs(init), abs(null))}$$

and for null points it is defined as

$$N = \frac{null - init}{\max(abs(init), abs(null))}.$$

Variables that are negative by convention, specifically CIN and omega, will have positive normalized differences when initiation values are less negative (smaller in magnitude) than null values. Variables that are always of one sign will have values of *I* and *N* that are always between -1 and 1. For variables that have meaningful values of either sign, *I* and *N* are bound by -2 and 2. For both types of variables, the distribution of normalized differences for the null points is symmetric about 0 with respect to the normalized differences for initiation points. The above formulation is still vulnerable to both initiation and null values being zero. In these situations the normalized difference is set to 0.

Because not all the null points could be paired with an initiation point (due to the MUCAPE criterion), the number of pairs considered in this step of the analysis is a bit less than the number of null points at each range. The number of pairs ranges from 315,000 at 60 km to 340,000 at 180 km. The box-and-whisker plots of *I* and *N* for each parameter are shown in Figs. 5-6, where the number following *I* or *N* corresponds to the range (60, 120, or 180 km).

Like the raw values, the discriminatory ability of each parameter increases with greater separation between initiation and null points. Also, the best-performing parameters still appear to be maximum omega, Δz*, convergence, MLCAPE, and MLCIN. One attribute of the convergence distributions that is worth noting is that even though the medians are separated by a considerable amount, the area of overlap between the boxes is quite large. Plotting a histogram of the values of *I* for 0-LFC convergence at 120 km shows that the distribution is bimodal (Fig. 7). This bimodality is common to both convergence parameters at all distances. The larger peak is the positive one, and more than half of the values are positive, which is why the median is significantly positive. However, there are a lot of negative values as well, which is why the third quartile is not higher. The bimodality means that convergence values at initiation and null points are not very well correlated, suggesting a field that is noisy rather than smoothly varying. This enhances the possibility of getting unrepresentative raw or normalized difference values for convergence if the RUC places a convergent boundary incorrectly, even if the error is fairly slight.

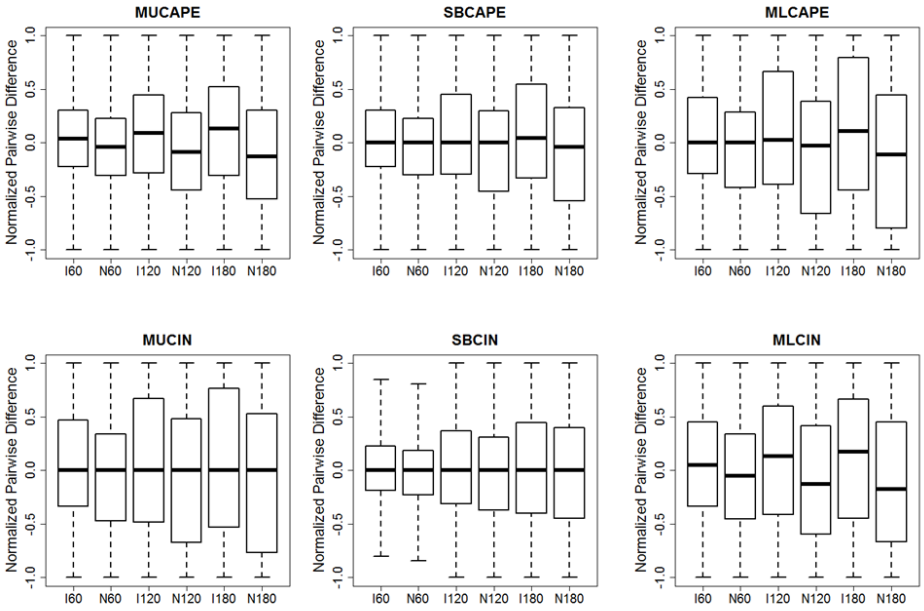

Figure 5: Normalized pairwise difference distributions of CAPE and CIN at 60, 120, and 180 km.

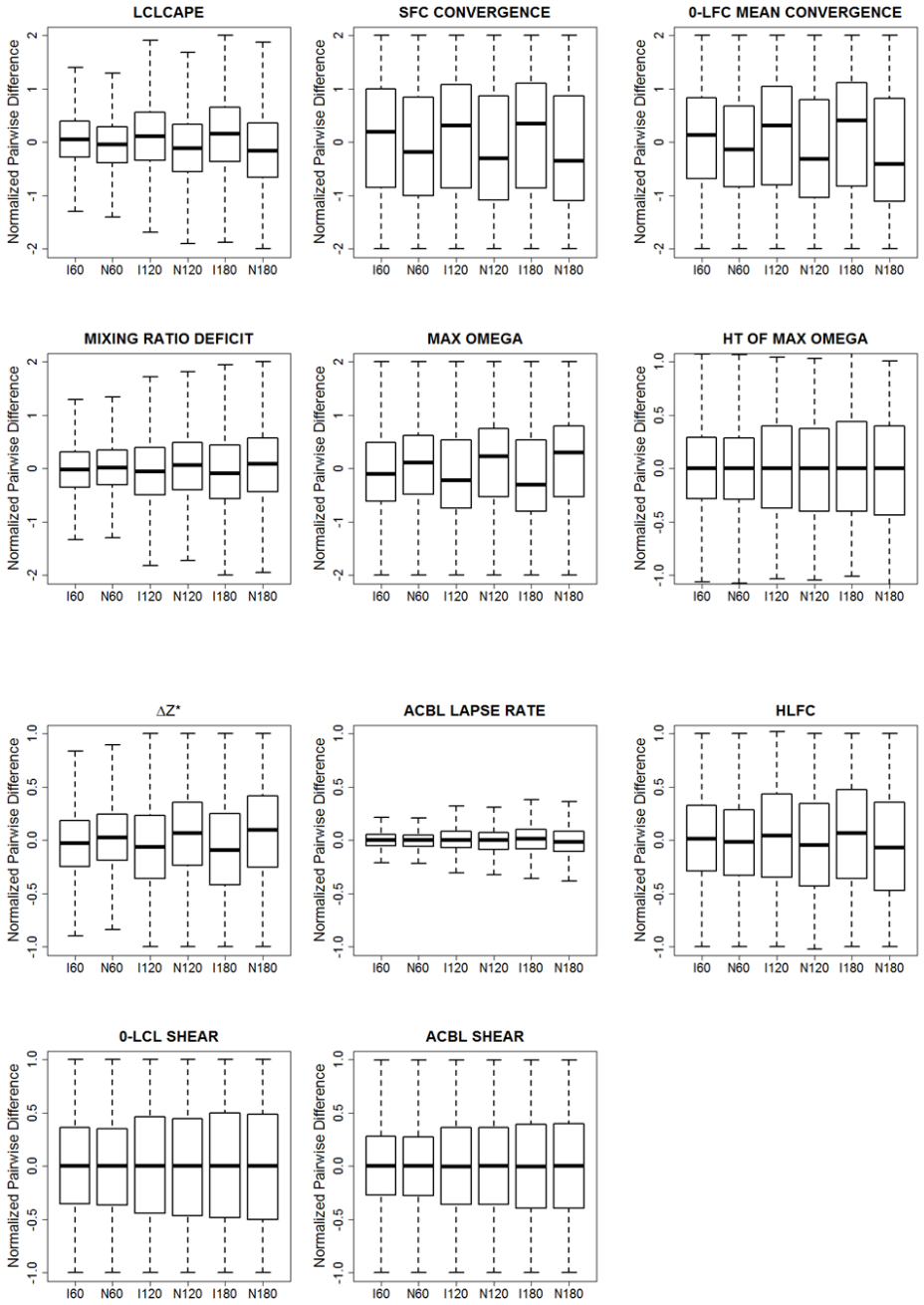

Figure 6: Normalized pairwise difference distributions at 60, 120, and 180 km for remaining parameters.

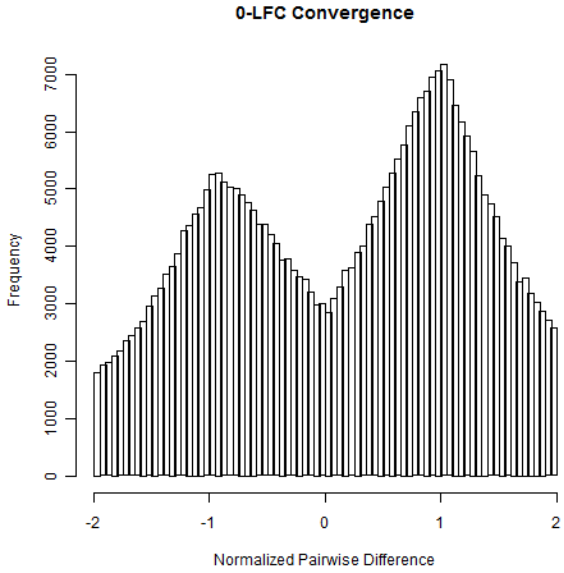

Figure 7: Histogram of normalized differences in 0-LFC convergence for initiation points at 120 km.

The ultimate goal of this work is to provide insight on which of the relevant factors for convection is most often the one missing from cases of initiation failure. In order to provide this insight, the frequency of normalized differences that are "significantly" positive or negative for each parameter are cataloged in order to see how many of the initiation/null pairs could be correctly identified by various combinations of parameters. To "correctly identify" the pair of points is to be able to find parameters with significant differences of a sign consistent with initiation at the initiation point rather than the null point. Differences were determined to be "significant" if they were outside the overlapping part of the boxes on the box-and-whisker plots. Mathematically, the significance threshold is $T = \min\{q_{3,init}, q_{3,null}\}$, where $q_{3,init}$ and $q_{3,null}$ are the upper quartile for the initiation and null distributions, respectively. This threshold is determined for each variable at each range. If the absolute value of a normalized difference is greater than *T* for that variable, then the sign of the normalized difference is cataloged. Variables with better separation in the distributions will have a greater number of significant differences, and a greater percentage of them should be of the same sign.

The first step in finding the parameters offering the best discrimination of initiation and null environments is to rank the parameters based the percentage of significant differences that are of the same sign using the entire dataset. The rankings shown in Table 4 are based on the 120 km range, and as with the separation values shown in Table 3, the values increase with range but the ranking is the same.

Table 4: Ranking of parameters by significant differences over the entire dataset at the 120 km range.

Parameter	**% of significant differences of same sign**	**Abs(# Pos. differences – # Neg. differences)**
Maximum omega	59.56	39885
MUCAPE	59.01	37154
MLCAPE	58.90	36587
LCLCAPE	58.89	36547
MLCIN	58.66	24809
0-LFC convergence	58.41	34202
Δz*	57.95	31294
Sfc convergence	57.56	30013
SBCAPE	57.03	27649
H_{LFC}	54.84	18106
MUCIN	54.75	17737
MRD	54.53	16830
ACBL lapse rate	53.68	13394
SBCIN	51.52	4320
Ht of max omega	51.48	5167
Subcloud shear	51.10	3815
ACBL shear	50.03	116

It is likely that several of the parameters in Table 4 are closely related to other parameters near them in the list. For example, all the CAPE and CIN values should be correlated, since they are all derived from the same basic procedure applied to the same sounding. Likewise, omega and convergence (especially 0-LFC mean convergence) are dynamically linked via the continuity equation, so when one is favorable the other should be as well – they are largely redundant. Also, since mixing ratio deficit is an integrated quantity, and the depth of integration depends on Δz*, they are related. And of course H_{LFC} is derived from the height of maximum omega and Δz*, so they will be related.

To account for the interrelatedness of the parameters, the procedure for determining which ones

are most useful is to start the list with the one that is most effective for all the data, in this case maximum omega. Then the same procedure that was applied to get Table 4 is applied to cases in which maximum omega is not significant to find the next important parameter. This is done recursively until no more useful parameters are left. When one parameter is controlled for, other parameters strongly linked with it should be largely controlled for as well. This is more effective than simply comparing the effectiveness of the parameters based on all the data, as it is difficult to say for certain which one of a set of related parameters is really best.

Implementation of this procedure at each range determined that the three best parameters are maximum omega, MLCAPE, and Δz*. After those were accounted for, the next best parameter was 0-LFC convergence, which is directly related to omega, which we have already used. This suggests that all the truly important factors have been accounted for.

With the list of parameters narrowed to three, it is possible to evaluate how often each one is the one that is different when the other two are neutral. These results are presented both as conditional probabilities and total number of occurrences, as the number of cases with the other two parameters both neutral was not necessarily the same (Table 5). Specifically, the number of cases with two of the three parameters neutral decreased with range. Since lower values of omega and Δz* favor initiation, the conditional probability evaluated is the probability of a significant negative difference given that the other two parameters are neutral, whereas for MLCAPE it is the probability of a significant positive difference given the same condition. From these calculations, maximum omega was the most significant parameter. The conditional probabilities of a significant difference in the "correct" direction are slightly higher at the 180 km range, and slightly lower at the 60 km range, though the relative importance of each factor is the same. This suggests that it is simply the model detecting fewer differences between points that are closer together, which is unsurprising.

Parameter values were also collected at initiation and null points an hour before the time of initiation. Examination of these values showed that the only measurable difference between the two times (determined by using pairwise differences between the t_0 and t_{-1} data) is a slight increase in upward motion and convergence at the initiation points.

Table 5: Conditional probabilities of "correct" significant differences (count of such occurrences in parentheses) at each range.

Parameter	60 km	120 km	180 km
Max omega	30.46 (19645)	35.57 (20409)	39.9 (20463)
MLCAPE	28.41 (17587)	32.23 (17049)	34.62 (15554)
Δz*	28.51 (17559)	31.85 (16576)	34.14 (14869)

5. DISCUSSION

The parameters consistently identified as most important in this work are maximum omega, Δz*, and CAPE. All of the CAPE parameters are highly correlated, and when one of them is selected as the best parameter, the others are usually not far behind, so whether MUCAPE or MLCAPE is selected as "best" may not be tremendously significant. Both of them are primarily measures of buoyancy, though MLCAPE also accounts for dilution, which MUCAPE does not. Since SBCAPE is either equivalent or inferior to MUCAPE (depending whether the convection is surface-based or elevated), and it lacks the ability of MLCAPE to account for dilution, there is not a situation in which SBCAPE is the best one to use for evaluating the potential for thunderstorm initiation.

Relating these parameters back to the four basic factors indicates that lift is the most important single factor in determining where thunderstorms will initiate. Physically, it makes sense that lift would be most important factor. In addition to its role as a trigger for thunderstorm initiation, upward motion also serves a role in preconditioning the atmosphere. Persistent updrafts along a boundary act to deepen the moist boundary layer, making it more suitable for subsequent updrafts to reach their LFC (Ziegler et al. 1997). Since both lift and inhibition were measured, it is apparent from these results that initiation failures due to "insufficient" lift are more commonly due to differences in lift rather than differences in inhibition. Also, buoyancy appears to be a more important factor than dilution, although both MLCAPE and Δz* have a relationship to dilution. The criterion that all points used in the analysis have positive MUCAPE already controlled for buoyancy to a limited degree. While this may result in a slight underestimation of the importance of buoyancy, cases

where thunderstorms failed to initiate due to an absence of buoyancy are trivial.

Since deep convection is parameterized in the model used to compute the environmental parameters, there may be some concern about the values for maximum omega in this study actually representing the effects of the convective parameterization being triggered at the gridpoint chosen to represent initiation (it is an initiation point after all). It appears unlikely that this is a significant influence on the results for a number of reasons. First, the vertical domain for finding the maximum omega extends to at most 100 mb above the LFC, so the highest midlevel updraft values should not be sampled. Also, if the convective parameterization was triggered, omega values should increase significantly above the LFC and the maximum omega value should occur at the upper bound of this domain. This should result in significant differences in the height of maximum omega compared to null points where the convective parameterization is not active. It should also result in H_{LFC} values significantly above 1. However, neither of these is true about the dataset in general, as height of maximum omega shows essentially no difference between initiation and null points, and the median H_{LFC} value is very near 1. Additionally, only a very slight increase in the omega value is noted in the hour prior to initiation, which is not consistent with a change in the status of the convective parameterization. Though it is impossible to rule out the possibility of the convective parameterization coming into play in a few cases, it seems reasonable to conclude that the differences in omega are legitimate variations in the environment rather than artifacts of the model convective parameterization.

The interrelatedness of the parameters used here shows that the initiation of deep convection is a complex process that cannot easily be boiled down to a single number. A value of a certain parameter, such as omega, that might support initiation in one environment may not in another, since the distance to the LFC or some other parameter is different. Also, a wide range of thermodynamic environments are capable of initiating deep convection, which makes the creation of parameters that apply to all thunderstorms difficult. Defining parameters that use layers dependent on the parcel LCL or LFC to make them adaptable to different thermodynamic environments ends up introducing unintended interdependencies, and a parameter intended to measure one thing becomes dependent on something else. For example, the mixing ratio deficit and ACBL lapse rate are mainly intended to measure dilution or the feedback between buoyancy and dilution, though both of them are sensitive to Δz^*, since the location of the LFC determines what layer is considered in evaluating them. When using parameters defined in such a way, it is important to keep these interdependencies in mind.

The goal of this study was to identify which parameters (and ultimately processes) are most important to the initiation of thunderstorms in real-world environments. The relevance to forecasting is helping distinguish the parameters that are useful from the ones that are not, as well as identifying relationships between different parameters that may be relevant to their interpretation. It is beyond the scope of this work to determine the best algorithm to forecast thunderstorm initiation using these parameters. However, some suggestions can be offered. The way to translate the pairwise difference approach to something computable on a grid is most likely through the evaluation of differences from a neighborhood mean. This study can offer some guidance on an appropriate radius over which to compute the spatial mean. These values could be used as “interest fields” or as input to a number of decision-making techniques, including decision trees and logistic regression.

6. CONCLUSIONS

The goal of this work is to determine which of the four basic factors (lift, inhibition, buoyancy, and dilution) that regulate convection is most often responsible for initiation or non-initiation. This is done using parameters derived from 20-km RUC-II analysis near a large sample of thunderstorm initiation points and null points. Analysis of the raw parameter values showed that a wide range of environments are capable of initiating convection and as a result there are no “magic numbers” that effectively discriminate initiation and null points. Neither subcloud shear nor ACBL shear show any meaningful differences between initiation and null environments. However, the orientation of the shear with respect to a possible initiating boundary was not considered, and this is likely important for the shear in both layers.

Analysis of pairwise differences between initiation and null points shows that lift is the most important single factor, and that the maximum upward motion in the column (no higher than 100 mb above the LFC) is the most effective way to quantify lift. The two next most effective parameters are MLCAPE (measuring

buoyancy) and Δz* (measuring inhibition). Beyond these three parameters, there is not much additional information to be gained in remaining parameters. Even though none of those parameters primarily related to dilution, that does not mean that it can be ignored. The primary value of MLCAPE over MUCAPE or SBCAPE is that it attempts to include the effects of dilution, and the distance a parcel has to travel (Δz*) influences the amount of dilution a parcel can experience below the LFC. Greater lift facilitates initiation through preconditioning as well as triggering, so it makes sense that lift would be the most significant factor and dilution would be of secondary importance.

ACKNOWLEDGEMENTS

This work was supported by NSF Grant AGS-0757189 and utilized computing resources at the Holland Computing Center at the University of Nebraska.

References

Banacos, P.C., and D.M. Schultz, 2005: The Use of Moisture Flux Convergence in Forecasting Convective Initiation: Historical and Operational Perspectives. *Wea. Forecasting*, **20**, 351-366.

Benjamin, S.G, and Coauthors, 2004: An Hourly Assimilation-Forecast Cycle: The RUC. *Mon. Wea. Rev.*, **132**, 495-518.

Craven, J.P, R. Jewell, and H. Brooks, 2002: Comparison Between Observed Convective Cloud-Base Heights and Lifting Condensation Level for Two Different Lifted Parcels. *Wea. Forecasting*, **17**, 885-890.

Doswell, C.A III, and E.N. Rasmussen, 1994: The Effect of Neglecting the Virtual Temperature Correction on CAPE Calculations. *Wea. Forecasting*, **9**, 625-629.

--------, and D.M. Schultz, 2006: On the Use of Indices and Parameters in Forecasting Severe Storms. *Electronic J. Severe Storms Meteor.*, **1**(3), 1-22.

Houston, A.L., and D. Niyogi, 2007: The Sensitivity of Convective Initiation to the Lapse Rate of the Active Cloud-Bearing Layer. *Mon. Wea. Rev.*, **135**, 3013-3032.

Johns, R.H., and C. Doswell, 1992: Severe Local Storms Forecasting. *Wea. Forecasting*, **7**, 588-612.

Lakshmanan, V., T. Smith, K. Hondl, G. Stumpf, and A. Witt, 2006: A Real-Time, Three-Dimensional, Rapidly Updating, Heterogeneous Radar Merger Technique for Reflectivity, Velocity, and Derived Products. *Wea. Forecasting*, **21**, 802-823.

--------, A. Fritz, T. Smith, K. Hondl, and G. Stumpf, 2007a: An Automated Technique to Quality Control Radar Reflectivity Data. *J. Appl. Meteor. Climatol.*, **46**, 288-305.

--------, T. Smith, G. Stumpf, and K. Hondl, 2007b: The Warning Decision Support System – Integrated Information. *Wea. Forecasting*, **22**, 596-612.

--------, K. Hondl, and R. Rabin, 2009: An Efficient, General-Purpose Technique for Identifying Storm Cells in Geospatial Images. *J. Atmos. Oceanic Technol.*, **26**, 523-537.

Lahowetz, J., A. Houston, G. Limpert, A. Gibbs, and B. L. Barjenbruch, 2010: A Technique for Developing a U.S. Climatology of Thunderstorms: The ThOR Algorithm. *Proc. 25th Conf. on Severe Local Storms*, Denver, CO, Amer. Meteor. Soc., 16B.1.

Lee, B.D., R.D. Farley, and M.R. Hjelmfelt, 1991: A Numerical Case Study of Convection Initiation along Colliding Convergence Boundaries in Northeast Colorado. *J. Atmos. Sci.*, **48**, 2350-2366.

Markowski, P., C. Hannon, and E. Rasmussen, 2006: Observations of Convection Initiation "Failure" from the 12 June 2002 IHOP Deployment. *Mon. Wea. Rev.*, **134**, 375-405.

Mesinger, F., and Coauthors, 2006: North American Regional Reanalysis. *Bull. Amer. Meteor. Soc.*, **87**, 343-360.

Moncrieff, M.W., and M.J. Miller, 1976: The Dynamics and Simulation of Tropical Cumulonimbus and Squall Lines. *Quart. J. Roy. Meteor. Soc.*, **102**, 373-394.

NCDC, North American Regional Reanalysis (NARR) for 2005-2007: *NOMADS Web Interface*, http://nomads.ncdc.noaa.gov, accessed Aug 2010.

--------, Rapid Update Cycle (RUC) 20 km grid for 2005-2007: *NOMADS Web Interface*, http://nomads.ncdc.noaa.gov, accessed Aug 2011.

--------, Level-II NEXRAD Data for 2005-2007: *HDSS Access System*, http://has.ncdc.noaa.gov, accessed Dec 2011.

Peckham, S.E., and L.J. Wicker, 2000: The Influence of Topography and Lower-Tropospheric Winds on Dryline Morphology. *Mon. Wea. Rev.*, **128**, 2165-2189.

Purdom, J.F.W., 1982: Subjective Interpretations of Geostationary Satellite Data for Nowcasting. *Nowcasting*, K. Browning, Ed., Academic Press, 149-166.

Rotunno, R., J.B. Klemp, M.L. Weisman, 1988: A Theory for Strong, Long-Lived Squall Lines. *J. Atmos. Sci.*, **45**, 463-485.

Stull, R.B., 1985: A Fair-Weather Cumulus Cloud Classification Scheme for Mixed-Layer Studies. *J. Climate Appl. Meteor.*, **24**, 49-56.

Thompson, R.L, R. Edwards, J. Hart, K. Elmore, and P. Markowski, 2003: Close Proximity Soundings within Supercell Environments Obtained from the Rapid Update Cycle. *Wea. Forecasting*, **18**, 1243-1261.

Weisman, M.L., and J.B. Klemp, 1982: The Dependence of Numerically Simulated Convective Storms on Wind Shear and Buoyancy. *Mon. Wea. Rev.*, **110**, 504-520.

Wilson, J.W., and W.E. Schreiber, 1986: Initiation of Convective Storms at Radar-Observed Boundary- Layer Convergence Lines. *Mon. Wea. Rev.*, **114**, 2516-2536.

--------, G.B. Foote, N.A. Crook, J.C. Fankhauser, C.G. Wade, J.D. Tuttle, C.K. Mueller, and S.K. Kreuger, 1992: The Role of Boundary-Layer Convergence Lines and Horizontal Rolls in the Initiation of Thunderstorms: A Case Study. *Mon. Wea. Rev.*, **120**, 1785-1815.

--------, and R. Roberts, 2006: Summary of Convective Storm Initiation and Evolution during IHOP: Observational and Modeling Perspective. *Mon. Wea. Rev.*, **134**, 23-47.

Xue, M., and W.J. Martin, 2006: A High-Resolution Modeling Study of the 24 May 2002 Dryline Case during IHOP. Part II: Horizontal Convective Rolls and Convective Initiation. *Mon. Wea. Rev.*, **134**, 172-191.

Ziegler, C.L., T.J. Lee, and R.A. Pielke Sr., 1997: Convective Initiation at the Dryline: A Modeling Study. *Mon. Wea. Rev.*, **125**, 1001-1026.

--------, and E.N. Rasmussen, 1998: The Initiation of Moist Convection at the Dryline: Forecasting Issues from a Case Study Perspective. *Wea. Forecasting*, **13**, 1106-1131.